

## Breakup of oxygen nucleus on isotopes of hydrogen and nitrogen nuclei in collisions with protons at $3.25A$ GeV/c

Kosim Olimov\*, Khusniddin K. Olimov\*,<sup>†,‡,¶</sup>, Sagdulla L. Lutpullaev\*,  
Alisher K. Olimov\*, Vladimir V. Lugovoi\*,  
Vadim Sh. Navotny\* and Bekhzod S. Yuldashev<sup>§</sup>

*\*Physical Technical Institute of SPA Physics  
Sun Of Uzbek Academy of Sciences, Tashkent, Uzbekistan*

*<sup>†</sup>Inha University in Tashkent, Tashkent, Uzbekistan*

*<sup>‡</sup>Department of Physics,  
COMSATS Institute of Information Technology,  
Islamabad, Pakistan*

*<sup>§</sup>Joint Institute for Nuclear Research, Dubna, Russia  
<sup>¶</sup>drolimov@gmail.com*

Received 5 March 2016

Revised 17 June 2016

Accepted 18 June 2016

Published 28 July 2016

Phenomenological analysis of breakup of oxygen nuclei on fragments with the charges one and seven in collisions with protons at  $3.25A$  GeV/c was conducted using the Monte Carlo model of isotropic phase space. For the first time, the contributions of mechanism of diffractive breakup of oxygen nucleus and that of quasi-elastic knocking out of one of the protons of oxygen nucleus by a proton target into channel of formation of proton fragment and  $^{15}\text{N}$  nucleus with conservation of recoil proton in final state were determined. Cross-section of diffractive breakup of oxygen  $^{16}\text{O}$  nucleus on  $^{15}\text{N}$  nucleus and proton fragment and that of diffractive breakup of  $^{16}\text{O}$  nucleus on nuclei  $^{14}\text{N}$  and  $^2\text{H}$  were estimated for the first time in  $^{16}\text{O}p$  collisions at  $3.25A$  GeV/c.

*Keywords:* Fragmentation of nuclei; structure of nuclei; excitation of nuclei; formation of light nuclei.

PACS Number(s): 25.10.+s, 27.20.+n

### 1. Introduction

Investigation of peripheral collisions of light nuclei allows one to obtain unique information about the excited states of nuclei above the energy threshold of their

<sup>¶</sup>Corresponding author.

breakup on nucleons. Peripheral interactions are characterized by formation of narrow jets of fragments of incident nucleus with the total charge and baryon number being close to those of impinging nucleus. It is clear that nuclei participating in such interactions acquire quite low excitation energies, close to energy thresholds for breakup into various configurations of nuclear fragments. For light and medium nuclei, the structures such as  $n\alpha$ ,  $n\alpha + md$ ,  $n\alpha + mt$  and  $n\alpha + m^3\text{He}$  (here  $n \geq 1$  и  $m \geq 1$ , and they depend on mass number and type of fragmenting nucleus<sup>1-5</sup>) are observed. Data on cross-sections of formation of such structures have practical application in solving the problems of nuclear astrophysics, and can also be used for scenarios of nucleon synthesis, based on coalescence of various cluster structures.

This work is devoted to detailed analysis of breakup of oxygen nuclei into fragments with the charges one and seven in interactions with protons at  $3.25A\text{ GeV}/c$ . The main aim of this paper is to obtain valuable information on mechanisms of breakup of oxygen nuclei on isotopes of hydrogen and nitrogen nuclei in collisions with protons at  $3.25A\text{ GeV}/c$ .

In experiment, all the theoretically possible topologies with the total charge of multicharged fragments (with  $z \geq 2$ ) equal to seven, i.e., topologies (223), (34), (25), and (7) are observed (here the single digits denote the charges of multicharged fragments, and their number is the total number of such fragments in a collision event). Among these topologies, the maximal yield cross-section belongs to topology (7) –  $65.35 \pm 1.47\text{ mb}$ , and the minimal yield cross-section is observed for topology (34) –  $0.66 \pm 0.15\text{ mb}$ .<sup>6</sup> Therefore, we analyze the channels of breakup of oxygen nuclei onto fragments with the charges one and seven i.e., the topology (7), in this work. Here the topology (7) events are those  $^{16}\text{Op}$  collisions at  $3.25A\text{ GeV}/c$ , which contain, besides singly charged particles, one fragment with the charge  $Z = 7$  in final state. We will study the mean multiplicities of particles accompanying the fragment with the charge  $Z = 7$  to obtain new information about mechanism of realization of topology (7) events in  $^{16}\text{Op}$  collisions at  $3.25A\text{ GeV}/c$ . To learn about the role of charge exchange processes between a target proton and impinging oxygen nucleus in events of topology (7), the average value of the total charge of all the charged fragments of oxygen nuclei will also be determined for such events.

The present work is organized as follows. The experimental procedures are given in Sec. 2. Section 3 is devoted to analysis of general characteristics of events of topology (7) in  $^{16}\text{Op}$  collisions at  $3.25A\text{ GeV}/c$ . Analysis of three prong events (i.e., with three charged fragments (particles) in final state) of topology (7) is presented in Sec. 4. Summary and conclusions are given in Sec. 5.

## 2. Experimental Procedures

The experimental data were obtained using 1 m hydrogen bubble chamber of the Laboratory of High Energies (LHE) of Joint Institute for Nuclear Research (JINR), irradiated by oxygen nuclei having momenta of  $3.25A\text{ GeV}/c$ , accelerated at Dubna synchrophasotron, and consist of 8712 fully measured inelastic  $^{16}\text{Op}$  collision events.

For identification of mass of the fragments, the following momentum intervals in laboratory frame were introduced. Singly charged fragments with  $1.75 \text{ GeV}/c < p \leq 4.75 \text{ GeV}/c$  were considered to be protons, those with  $4.75 \text{ GeV}/c < p \leq 7.75 \text{ GeV}/c$ , and  $p > 7.75 \text{ GeV}/c$  were taken to be  $^2\text{H}$  and  $^3\text{H}$  nuclei, respectively. Fragments having the charge of seven and belonging to momentum intervals  $p \leq 43.8 \text{ GeV}/c$ ,  $43.8 \text{ GeV}/c < p \leq 47.1 \text{ GeV}/c$ , and  $p > 47.1 \text{ GeV}/c$  were taken to be  $^{13}\text{N}$ ,  $^{14}\text{N}$ , and  $^{15}\text{N}$  nuclei, respectively.<sup>7-10</sup> At such a selection, the admixture of neighboring isotopes among selected fragments due to overlap of their momentum spectra does not exceed 5%.<sup>7</sup> Such a separation of fragments by their charge and mass allows one to determine the multiplicity of bound neutrons in multicharged fragments in each individual collision event. Since the number of bound protons in the studied topology (7) equals to eight, it is also possible to determine the multiplicity of unbound neutrons using the law of conservation of electrical and baryon charges.

The methodical peculiarities of 1 m hydrogen bubble chamber of JINR allow one to separate unambiguously tracks of  $\pi^+$  mesons and protons in momentum region  $p < 1.25 \text{ GeV}/c$  in laboratory frame.<sup>7</sup> Their separation in momentum interval  $1.25 < p < 1.75 \text{ GeV}/c$  was made according to a procedure described in Ref. 11, which allowed to measure more precisely the mean multiplicities of proton fragments, neutron fragments,  $\pi^+$  mesons, and recoil proton along with obtaining useful information about the charge exchange processes.

### 3. General Characteristics of Events of Topology (7)

Let us consider the mean multiplicities per event of charged pions, recoil proton ( $p_r$ ), and singly charged fragments ( $^1\text{H}$ ,  $^2\text{H}$ ,  $^3\text{H}$ ) in events of topology (7), which are given in Table 1.

As seen from Table 1, the proton fragments have the maximum mean multiplicity among the singly charged fragments, which is due to selection criterion of events with formation of fragment with the charge of seven in final state. In other words, due to selection criterion of events of topology (7), an oxygen nucleus should lose one singly charged fragment in a collision event. Loss of a singly charged fragment of an oxygen nucleus can occur via the direct knocking out of one of the protons of oxygen nucleus by a target proton, or through a mechanism of “evaporation”. It is also seen that the mean multiplicity of recoil proton is close to that for proton fragments, which is due to dominant contribution of  $pp$  collisions to formation of a fragment

Table 1. The mean multiplicities per event of charged pions, recoil proton ( $p_r$ ), and singly charged fragments ( $^1\text{H}$ ,  $^2\text{H}$ ,  $^3\text{H}$ ) for all events of topology (7).

Type of a particle or fragment					
$^1\text{H}$	$^2\text{H}$	$^3\text{H}$	$p_r$	$\pi^+$	$\pi^-$
$0.82 \pm 0.01$	$0.032 \pm 0.004$	$0.004 \pm 0.002$	$0.78 \pm 0.01$	$0.54 \pm 0.01$	$0.18 \pm 0.01$

of oxygen nucleus with the charge of seven in final state. Quite small probability of formation of deuteron and tritium nuclei together with one of the isotopes of nitrogen nuclei is caused by peripheral character of realization of topology (7).

As will be shown below, a part of deuterons can be formed due to a diffractive breakup of oxygen nucleus through a channel  $^{16}\text{O} + p \rightarrow ^{14}\text{N} + ^2\text{H} + p$ .

As seen from Table 1, the mean multiplicity of positive pions is practically three times larger than that of negative pions. This is, as mentioned above, due to a dominant contribution of  $pp$  collisions in events of topology (7). At such a collision, both target proton and proton fragment can transform with a certain probability into neutron and positive pion through inelastic charge exchange reaction, which is a supplementary source of  $\pi^+$  production. Quite small mean multiplicity of negative pions can also be explained by an absence of  $\pi^-$  in events with three charged particles in final state (including fragments with the charges one and seven) due to conservation law of electric charge.

It is of interest to determine the average value of the total charge of all the fragments (including fragments with the charges one and seven) of oxygen nucleus in events of topology (7). It is easy to show, using the data of Table 1 and event selection criteria, that the average charge of all fragments of oxygen nucleus in topology (7) equals  $7.86 \pm 0.01$ . Using cross-sections of yield of isotopes of nitrogen nuclei<sup>12</sup> in  $^{16}\text{O}p$  collisions at  $3.25A \text{ GeV}/c$  and data of Table 1, we calculated the mean multiplicities of bound and unbound neutrons in topology (7), which proved to be  $7.36 \pm 0.04$  and  $0.78 \pm 0.04$ , respectively. Subtracting the mean multiplicity of proton fragments from the average charge of all fragments of oxygen nucleus in topology (7), the mean multiplicity of bound protons was measured to be  $7.04 \pm 0.02$ . Even though the mean multiplicities of unbound proton fragments and unbound neutrons coincided within statistical uncertainties, the mean multiplicity of bound protons proved to be notably smaller than that of bound neutrons, which is certainly due to event selection criteria of topology (7).

Let consider the distribution of events of topology (7) on the total charge  $Q = \sum Z_f$  of all fragments for a detailed analysis of the processes of increasing or decreasing of an initial charge of oxygen nucleus. The distribution of events of topology (7) on the total charge  $Q = \sum Z_f$  of all fragments is presented in Table 2. Five events were excluded from the total statistics of 1546 events, because it was not feasible to correctly restore the momenta of the fragments, which underwent the secondary collisions, in these events. As seen from Table 2, the quantity  $Q$  varies from 7 to 10. The lower threshold is due to event selection of topology (7), corresponding

Table 2. Distribution of events of topology (7) on the total charge  $Q$  of all the fragments of oxygen nucleus.

The total charge ( $Q$ ) of all the fragments of oxygen nucleus				
7	8	9	10	All
$401 \pm 20$	$974 \pm 31$	$157 \pm 13$	$9 \pm 3$	$1541 \pm 39$

to a case when one of the protons of excited oxygen nucleus decays into neutron and positive pion. Indeed, the mean multiplicity of positive pions at  $Q = 7$  proved to be maximal and equal to  $1.24 \pm 0.02$ . The distribution on  $Q$  exhibits a maximum at  $Q = 8$  and minimum at  $Q = 10$ . The latter is connected with the following two processes: either the two neutrons of oxygen nucleus get excited and decay via charge exchange process into proton and negative pion (which is unlikely in peripheral interactions), or one of the excited neutrons decays into proton and negative pion, while the second one transforms into proton through acquiring the charge of a target proton. As expected, the mean multiplicity of negative pions proved to be maximal and equal to  $1.22 \pm 0.14$  at  $Q = 10$ , and that of recoil protons is minimal and equal to  $0.09 \pm 0.09$ . Hence, we can conclude that the events of topology (7) with  $Q = 10$  are realized predominantly due to inelastic charge exchange decay of one of the neutrons into proton and negative pion, and a transfer of a charge of target proton to one of the neutrons of oxygen nucleus.

Let consider now the distribution of events of topology (7) on the number  $n_{ch}$  of charged particles (including fragments of oxygen nucleus with the charges one and seven) in final state.

The distribution of events of topology (7) on the number  $n_{ch}$  of charged particles is presented in Table 3. As observed from Table 3, the maximal number of events of topology (7) is observed for three charged particles in final state (i.e., for three prong events), which makes up  $(83 \pm 2)\%$  of the total number of events, while the fraction of events with  $n_{ch} = 7$  in final state ( $(0.5 \pm 0.2)\%$ ) is negligibly small. The maximal fraction of three prong events in topology (7) is due to the peripheral character of realization of such events and the minimal energy threshold of this reaction as compared to reactions of topology (7) with formation of five and seven charged particles in final state.

It is of interest to study the influence of a charge exchange processes between a target proton and impinging oxygen nucleus as well as inelastic charge exchange of a target proton ( $p_r \rightarrow n + \pi^+$ ) in events of topology (7) on the energy threshold of a reaction, i.e., on the number of charged particles in final state. It is clear that the energy threshold of topology (7) events increases with an increase in the number of charged particles in final state. Therefore, we studied the dependence of the average number of a survived recoil proton on the number of charged particles in an event in topology (7).

The dependence of the average number of a survived recoil proton on the number of charged particles in an event in topology (7) is shown in Table 4. As seen from

Table 3. Distribution of events of topology (7) on the number  $n_{ch}$  of charged particles.

$n_{ch}$			
3	5	7	All
$1283 \pm 36$	$255 \pm 16$	$8 \pm 3$	$1546 \pm 39$

Table 4. Dependence of the average number of a survived recoil proton on the number of charged particles in an event in topology (7).

The number of charged particles in an event			
3	5	7	Total for topology (7)
$0.77 \pm 0.02$	$0.83 \pm 0.03$	$0.75 \pm 0.15$	$0.78 \pm 0.01$

Table 4, the mean multiplicity of a recoil proton does not depend within statistical uncertainties on the number of charged particles in an event and its average value for topology (7) proved to be  $0.78 \pm 0.01$  (see also Table 1). Hence, we can conclude that the processes of charge exchange between a target proton and impinging oxygen nucleus and inelastic charge exchange of a target proton ( $p \rightarrow n + \pi^+$ ) do not depend on the energy threshold of realization of topology (7) events.

Because the predominant fraction of events of topology (7) consists of three prong events with three charged particles in final state, further we will analyze in detail the characteristics of this group of events with the largest statistics.

#### 4. Analysis of Three Prong Events of Topology (7)

To understand more the mechanism of realization of three prong events of topology (7) events it is important to define the fraction of various nitrogen isotopes formed in such collisions. Moreover, it is of interest to compare these results for three prong events of topology (7) with the isotope composition of nitrogen nuclei formed in  $^{16}\text{O}p$  collisions at  $3.25A \text{ GeV}/c$  for all events of topology (7), determined earlier in Ref. 12. Table 5 presents the isotope composition of fragments with the charge seven in three prong events of topology (7), determined from approximation of experimental distribution on inverse momentum ( $x = 1/p$ ) of fragments with the charge seven by a sum of three Gaussian functions

$$\begin{aligned}
 F(x) = & a_1 * \exp(-b * (x - 1./(13. * 3.25))^2) \\
 & + a_2 * \exp(-b * (x - 1./(14. * 3.25))^2) + \dots \\
 & + a_3 * \exp(-b * (x - 1./(15. * 3.25))^2), \tag{1}
 \end{aligned}$$

where the quantities  $a_1/(a_1+a_2+a_3)$ ,  $a_2/(a_1+a_2+a_3)$ , and  $a_3/(a_1+a_2+a_3)$  characterize the relative contributions of the isotopes  $^{13}\text{N}$ ,  $^{14}\text{N}$ , and  $^{15}\text{N}$ , correspondingly. Here  $b = 1/(2\sigma^2)$  characterizes the width  $\sigma$  of a Gaussian distribution function. In Table 5, the statistical uncertainties of the fractions of different isotopes of nitrogen

Table 5. Isotope composition of fragments with the charge seven in three prong events of topology (7).

Fraction of isotopes of a nitrogen nucleus (%)		
$^{13}\text{N}$	$^{14}\text{N}$	$^{15}\text{N}$
$13.3 \pm 3.2$	$37.4 \pm 4.6$	$49.3 \pm 5.1$

nucleus were determined using the statistical uncertainties of parameters of approximation of experimental distribution by a sum of three Gaussian functions given in Eq. (1).

As seen from Table 5, the maximum yield in topology (7) is observed for isotope  $^{15}\text{N}$ , which is due to quite strong peripheral character of events in topology (7), where most of the events are due to a loss of one of the protons of oxygen nucleus. It is to be noted that the isotope composition of a nitrogen nucleus in three prong events coincided within statistical uncertainties with that obtained for all the events of topology (7) in Ref. 12. This is most probably due to the predominant contribution ( $(83 \pm 2)\%$ ) of three prong events to topology (7).

The mean multiplicities of proton fragments and  $\pi^+$  mesons in three prong events of topology (7) proved to be  $0.76 \pm 0.03$  and  $0.45 \pm 0.02$ , respectively. It is to be noted that the mean multiplicity of proton fragments in three prong events of topology (7) coincided within statistical uncertainties with that of a recoil proton (see Table 4). This fact points out to the predominant role of quasi-elastic scattering of a target proton on a proton of oxygen nucleus in three prong events of topology (7).

It is obvious that the proton fragments in topology (7) can be formed as a result of quasi-elastic knocking out of a proton of incident oxygen nucleus by a target proton, or through excitation of oxygen nucleus as a whole unit with subsequent emission of a proton through “evaporation” mechanism. These processes should be reflected in distribution on difference of azimuthal angles ( $\Delta\varphi(p_f p_r)$ ) of a proton fragment and target proton in the analyzed experimental events of topology (7). Figure 1 presents the experimental distribution on  $\Delta\varphi(p_f p_r)$  in events of topology (7).

As observed from Fig. 1, the distribution on  $\Delta\varphi(p_f p_r)$  is practically isotropic in region  $\Delta\varphi(p_f p_r) < 110^\circ$ , which is characteristic for a proton fragment formed due to mechanism of “evaporation” of excited oxygen nucleus. Furthermore, the

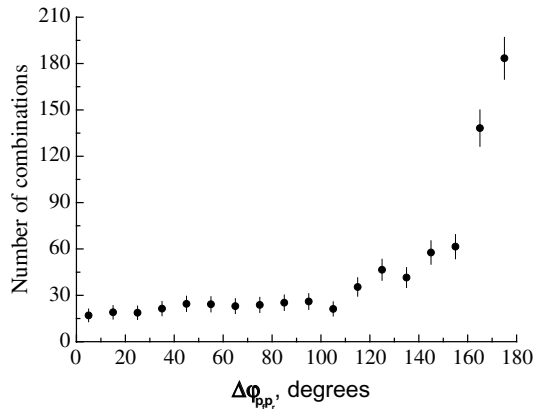


Fig. 1. Distribution on difference of azimuthal angles of a proton fragment and target proton in three prong events of topology (7).

spectrum on  $\Delta\varphi(p_f p_r)$  shows a weak rise and abrupt increase in regions  $110\text{--}160^\circ$  and  $\Delta\varphi(p_f p_r) > 160^\circ$ , respectively. Then the spectrum reaches its maximum at  $\Delta\varphi(p_f p_r) \approx 175^\circ$ , which points out the mechanism of quasi-elastic knocking out of a proton fragment by a target proton.

Hence, we can conclude that the proton fragments in three prong events of topology (7) are formed predominantly due to two mechanisms: quasi-elastic knocking out by a target proton and mechanism of “evaporation” of excited oxygen nucleus.

The shape of momentum spectrum of proton fragments in the rest frame of oxygen nucleus in topology (7), presented in Fig. 2, supports further the above conclusion. As seen from Fig. 2, the momentum spectrum of proton fragments exhibits a double structure shape: narrow peak at  $p \approx 80\text{ MeV}/c$  and small “shoulder” in region  $0.2 < p < 0.5\text{ GeV}/c$ . Further, the spectrum falls, extending up to momentum value of  $\sim 2\text{ GeV}/c$ . It is clear that the narrow peak of momentum spectrum is due to mechanism of “evaporation” of excited oxygen nucleus. The “shoulder” observed in region  $0.2 < p < 0.5\text{ GeV}/c$  is due to a mixture of contributions of two mechanisms of formation of proton fragments: “evaporation” mechanism and mechanism of quasi-elastic knocking out of a projectile proton by a target proton. The further fall of the spectrum in region  $p > 0.5\text{ GeV}/c$  is certainly due to the second mechanism mostly.

It is of interest to estimate the contributions of mechanism of quasi-elastic knocking out of a projectile proton by a target proton and mechanism of “evaporation” of the excited oxygen nucleus in formation of proton fragments in three prong events of topology (7). To solve this task, we considered the distribution on difference of azimuthal angles of a proton fragment and recoil proton in exclusive reaction



where  $p_f$  and  $p_r$  are proton fragment and recoil proton, respectively. The distribution on difference of azimuthal angles ( $\Delta\varphi(p_f p_r)$ ) of recoil proton and proton fragment for events of reaction in (2) is shown in Fig. 3.

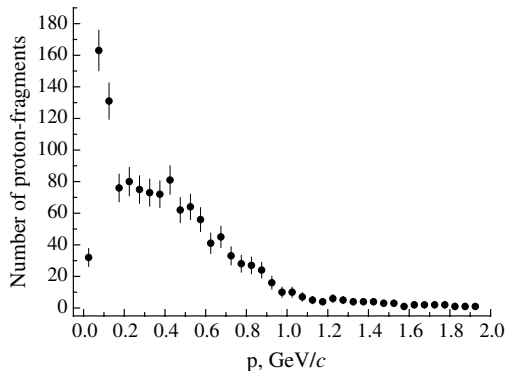


Fig. 2. Momentum spectrum of proton fragments in three prong events of topology (7) in system of rest of oxygen nucleus.



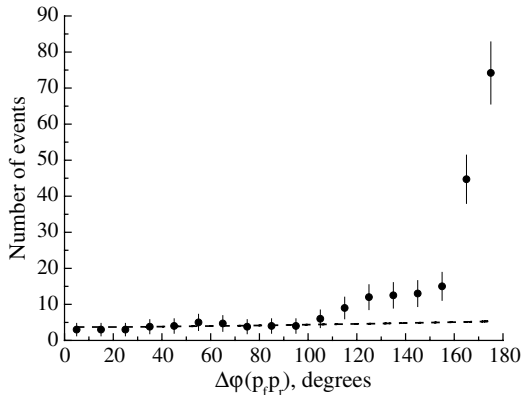


Fig. 3. Distribution on difference of azimuthal angles of a recoil proton and proton fragment in events of reaction in (2) (points: experiment; dashed curve: Monte Carlo calculations).

As seen from Fig. 3, the experimental spectrum on  $\Delta\varphi(p_f p_r)$  in region  $\Delta\varphi(p_f p_r) < 110^\circ$  shows a behavior, which is characteristic for protons originated from “evaporation” mechanism. The weak rise of the spectrum is observed in region  $110^\circ < \Delta\varphi(p_f p_r) < 160^\circ$ , which is seemingly due to smearing off of the spectrum due to Fermi momentum of a projectile proton, being close to a transferred momentum. Further, the spectrum abruptly increases in region  $\Delta\varphi(p_f p_r) > 160^\circ$ , reaching its maximum at  $\Delta\varphi(p_f p_r) = 175^\circ$ , which points out the mechanism of quasi-elastic knocking out of a proton fragment by a target proton.

To estimate the contributions of these mechanisms to a channel of oxygen breakup on proton fragment and  $^{15}\text{N}$  nucleus with conservation of a recoil proton in final state, we calculated the spectrum on difference of azimuthal angles of recoil proton and proton fragment within the framework of phenomenological Monte Carlo model of isotropic phase space.

In our Monte Carlo model calculations, we followed the algorithm and procedures described and used in Ref. 13 for reaction  $^{16}\text{O} + p \rightarrow ^{16}\text{O}^* + p_r \rightarrow ^4\text{He} + ^{12}\text{C} + p_r$ . Using the corresponding algorithm and procedures of Ref. 13, in this work we conducted Monte Carlo modeling of a reaction  $^{16}\text{O} + p \rightarrow ^{16}\text{O}^* + p_r \rightarrow ^{15}\text{N} + p_f + p_r$  (see Eq. (2)). Here we checked a hypothesis of diffractive formation of excited oxygen nucleus ( $^{16}\text{O}^*$ ) and its subsequent isotropic decay (in its rest frame) on  $^{15}\text{N}$  nucleus and proton fragment  $p_f$ . The aim of Monte Carlo calculations is to check a hypothesis that, as a result of diffractive interaction of impinging  $^{16}\text{O}$  nucleus with the target proton at rest, the oxygen nucleus gets excited as the whole and breaks up isotropically (in its rest frame). Then the deviation of experimental spectrum from calculated distribution will point out the existence of anisotropic processes (for example, knocking out of some nuclear structure (cluster) of oxygen nucleus by a proton target).

The three projections of momenta of recoil proton  $p_r$ , proton fragment  $p_f$ , and  $^{15}\text{N}$  nucleus were measured in 310 analyzed experimental events, which allowed to

calculate the invariant mass of an excited  $^{16}\text{O}^*$  nucleus in every experimental event. However, we do not know in advance whether it was isotropic decay of  $^{16}\text{O}^*$  nucleus in its rest frame. To test this assumption, we generated isotropic decay of  $^{16}\text{O}^*$  and, thus, obtained the theoretical energies and momenta of recoil proton  $p_r$ , proton fragment  $p_f$ , and  $^{15}\text{N}$  nucleus. Three projections of momenta of the excited  $^{16}\text{O}^*$  and impinging  $^{16}\text{O}$  nucleus permit to find the angles of three-dimensional space rotation and parameters of Lorentz transformation of energies and momenta of decay products ( $^{15}\text{N}, p_f$ ) from a system of rest of excited  $^{16}\text{O}^*$  nucleus to laboratory frame. For each of 310 experimental events, the invariant mass of  $^{16}\text{O}^*$  nucleus and transformation parameters from rest frame of  $^{16}\text{O}^*$  into laboratory system were determined. Then isotropic decay  $^{16}\text{O}^* \rightarrow (^{15}\text{N}, p_f)$  was generated (1000 times for each experimental event) and kinematic characteristics of decay products ( $^{15}\text{N}, p_f$ ) were transformed from rest frame of  $^{16}\text{O}^*$  into laboratory system. Hence, total 310,000 events were generated. All the details of Monte Carlo calculations can be found in early work.<sup>14</sup> The energy–momentum conservation was implemented with the relative precision of  $10^{-10}$  at all the stages of event generation.

In Fig. 3, the results of Monte Carlo model calculations are shown as the dashed curve. The calculated and experimental data were normalized in region  $\Delta\varphi(p_f p_r) \leq 110^\circ$ . The excess of the number of experimental events over the calculated spectrum in region  $\Delta\varphi(p_f p_r) > 110^\circ$  was found by subtracting the theoretical spectrum from the experimental distribution in this region. The excess of the number of experimental events over the calculated spectrum in region  $\Delta\varphi(p_f p_r) > 110^\circ$  can be referred to a mechanism of proton formation through the quasi-elastic knocking out of a projectile proton by a target proton.

The excess of the number of experimental events in region  $\Delta\varphi(p_f p_r) > 110^\circ$  proved to be  $206 \pm 14$ , corresponding to cross-section of  $8.7 \pm 0.6$  mb, and the number of events falling under the calculated spectrum was  $104 \pm 10$  with the corresponding cross-section of  $4.4 \pm 0.4$  mb. Hence, we can conclude that the main part ( $(66 \pm 5)\%$ ) of events in reaction (2) is realized through the quasi-elastic knocking out of a projectile proton by a target proton, and the remaining part ( $(34 \pm 5)\%$ ) can be referred to events of proton formation due to “evaporation” mechanism of an excited oxygen nucleus in peripheral interaction with a target proton. To estimate the cross-section of diffractive breakup of oxygen  $^{16}\text{O}$  nucleus on  $^{15}\text{N}$  nucleus and proton fragment, we introduced the following constraints, similar to those in Ref. 13, on emission angle and momentum of a recoil proton in laboratory frame:  $\theta_p > 70^\circ$ ,  $p_p < 0.4$  GeV/ $c$ . After introducing these constraints, there remained 125 events in reaction (2). Using the experimental distributions on three components of momenta of breakup products of reaction in (2) from these 125 experimental events, we generated 125,000 events according to Monte Carlo model, described above. To do this, we made Monte Carlo simulations of the three components of momenta of all decay products in reaction in (2) according to the corresponding experimental distributions on three components of momenta of these breakup products, taking into account the laws of conservation of momentum and energy in each of the

simulated events. More details on the simulation procedures according to Monte Carlo model of isotropic phase space can be found in our earlier work.<sup>13</sup> Then, the obtained theoretical spectrum on difference of azimuthal angles of a proton fragment and recoil proton was normalized with the corresponding experimental distribution in region  $\Delta\varphi(p_f p_r) \leq 110^\circ$ . The excess of the number of experimental events over the calculated spectrum in region  $\Delta\varphi(p_f p_r) > 110^\circ$  was found by subtracting the theoretical spectrum from the experimental distribution in this region. The excess of the number of experimental events in region  $\Delta\varphi(p_f p_r) \leq 110^\circ$  proved to be  $80 \pm 9$ , corresponding to cross-section of  $3.4 \pm 0.4$  mb, and the number of events falling under the calculated spectrum was  $47 \pm 7$  with the corresponding cross-section of  $1.9 \pm 0.3$  mb.

Hence, we can conclude that  $(15 \pm 2)\%$  of events in reaction (2) are realized as a result of diffractive breakup of excited (as a whole unit) oxygen nucleus in peripheral interaction with a target proton.

In topology (7), consisting of fully measured 1541 experimental events, the joint formation of a deuteron together with one of the isotopes of nitrogen nucleus is observed in 49 events only. Out of these 49 events, in 27 events the joint formation of a deuteron and  $^{14}\text{N}$  nucleus with conservation of a recoil proton in final state is observed, as given in reaction



These events can be considered as the candidates for diffractive breakup of oxygen nucleus on deuteron and nitrogen-14 nucleus. Due to small statistics of the events in reaction (3), it did not make sense to reconstruct the momentum and angular distributions of a recoil proton. In these events, the average values of emission angle and momentum of a recoil proton proved to be  $71 \pm 3^\circ$  and  $327 \pm 50$  MeV/c, respectively. For extraction of more realistic events of diffractive breakup of oxygen nucleus, we introduced the following constraints, similar to those in Ref. 13, on emission angle and momentum of a recoil proton in laboratory frame:  $\theta_p > 70^\circ$ ,  $p_p < 0.4$  GeV/c. After introducing such angular and momentum constraints, there remained 18 events (which make up  $\sim 2/3$  of the total number of events in reaction (3)) corresponding to cross-section of  $0.8 \pm 0.2$  mb. Quite a low cross-section of diffractive breakup of oxygen nucleus in reaction (3) could be explained as due to reconstruction of an initial  $\alpha$  cluster structure of oxygen nucleus and relatively small value of incident momentum per nucleon.

In Ref. 15, the cross-section of reactions  $^{12}\text{C} \rightarrow 2\alpha + 2d$  и  $^{12}\text{C} \rightarrow 2\alpha + t + p$  of coherent dissociation of carbon nuclei in  $^{12}\text{C} + ^{12}\text{C}$  collisions at  $4.2A$  GeV/c was estimated to be  $0.4 \pm 0.1$  mb. This cross-section proved to be more than ten times smaller than the cross-section of coherent dissociation of carbon nuclei ( $4.4 \pm 0.5$  mb) in reaction  $^{12}\text{C} \rightarrow 3\alpha$ , obtained under similar experimental conditions in Ref. 16. The cross-section of diffractive breakup of oxygen nucleus in reaction (3) in  $^{16}\text{O}p$  collisions at  $3.25A$  GeV/c, estimated in this work, proved to be of the same order of magnitude as the cross-section of coherent dissociation of carbon nuclei in reactions

$^{12}\text{C} \rightarrow 2\alpha + 2d$  и  $^{12}\text{C} \rightarrow 2\alpha + t + p$ , having energy thresholds of 31.2 and 27.1 MeV, respectively. Relatively larger cross-section of diffractive breakup of oxygen nucleus in reaction (3) is most probably due to lower energy threshold (20.7 MeV) of reaction  $^{16}\text{O} + p \rightarrow ^{14}\text{N} + ^2\text{H} + P_r$  compared to those in reactions  $^{12}\text{C} \rightarrow 2\alpha + 2d$  and  $^{12}\text{C} \rightarrow 2\alpha + t + p$ .

Hence, it can be concluded that the diffractive breakup of oxygen nucleus on  $^{14}\text{N}$  and  $^2\text{H}$  nuclei is observed in  $^{16}\text{O}p$  collisions at  $3.25A \text{ GeV}/c$ .

## 5. Summary and Conclusions

Analysis of channels of breakup of oxygen nuclei on fragments with the charges one and seven in interactions with protons at  $3.25A \text{ GeV}/c$  was conducted. It was observed that, among singly charged particles and fragments of oxygen nuclei, the proton fragments and recoil proton have the maximal multiplicity, which is due to selection criteria of events in topology (7) and peripheral character of the analyzed events. The mean multiplicities of proton fragments and recoil proton in topology (7) proved to be close to each other. This is because the main part of events of topology (7) is realized through quasi-elastic collision of a target proton with one of the protons of oxygen nucleus ( $pp$  collisions). The mean multiplicity of negative pions was three times smaller than that of positive pions. It is most probably due to the fact that, in events with three charged particles in final state (which make up  $(83 \pm 2)\%$  of the total number of events of topology (7)), production of  $\pi^-$  is not observed because of conservation law of electrical charge. Using Monte Carlo modeling of the exclusive reaction with nitrogen-15 nucleus and proton fragment with conservation of recoil proton in final state, we observed that the main fraction of proton fragments is formed due to quasi-elastic knocking out of one of the projectile protons by a target proton, while the remaining protons originate from “evaporation” mechanism of excited (as one whole unit) oxygen nucleus. Cross-section of diffractive breakup of oxygen  $^{16}\text{O}$  nucleus on  $^{15}\text{N}$  nucleus and proton fragment was estimated to be  $1.9 \pm 0.3 \text{ mb}$ .

Diffractive breakup of oxygen nucleus on nuclei  $^{14}\text{N}$  and  $^2\text{H}$  in  $^{16}\text{O}p$  collisions at  $3.25A \text{ GeV}/c$  was observed, where cross-section was estimated to be  $0.8 \pm 0.2 \text{ mb}$ . Cross-section of a channel of diffractive breakup of oxygen  $^{16}\text{O}$  nucleus on nuclei  $^{14}\text{N}$  and  $^2\text{H}$  proved to be approximately 2.5 times smaller than the corresponding cross-section of diffractive breakup of  $^{16}\text{O}$  nucleus on  $^{15}\text{N}$  nucleus and proton fragment. Such a difference in cross-sections of these two channels of diffractive breakup of oxygen nucleus is most probably due to significantly larger energy threshold (20.7 MeV) of reaction in (3) as compared to that (12.1 MeV) of reaction in (2).

## References

1. P. I. Zarubin, “Tomography” of the cluster structure of light nuclei via relativistic dissociation, in *Clusters in Nuclei*, Vol. 3, ed. C. Beck, Vol. 875 of the series Lecture Notes in Physics (Springer Verlag, New York, 2014), pp. 51–93.

2. N. P. Andreeva *et al.*, *Eur. Phys. J. A* **27** (2006) 295.
3. D. A. Artemenkov *et al.*, *Phys. At. Nucl.* **70** (2007) 1222.
4. T. V. Shedrina *et al.*, *Phys. At. Nucl.* **70** (2007) 1230.
5. M. Karabova *et al.*, *Phys. At. Nucl.* **72** (2009) 300.
6. K. N. Abdullaeva *et al.*, *Rep. Uzbek Acad. Sci.* **5** (1996) 21.
7. V. V. Glagolev *et al.*, *Eur. Phys. J A* **11** (2001) 285.
8. V. V. Glagolev *et al.*, *JETP Lett.* **58** (1993) 497.
9. V. V. Glagolev *et al.*, *JETP Lett.* **59** (1994) 336.
10. V. V. Glagolev *et al.*, *Yad. Fiz.* **58** (1995) 2005.
11. K. Olimov *et al.*, *Phys. At. Nucl.* **72** (2009) 596.
12. E. Kh. Bazarov *et al.*, *JETP Lett.* **81** (2005) 140.
13. K. Olimov *et al.* *Int. J. Mod. Phys. E* **25** (2016) 1650023.
14. V. M. Chudakov and V. V. Lugovoi, *Z. Phys. C* **59** (1993) 511.
15. V. V. Belaga *et al.*, *Phys. At. Nucl.* **60** (1997) 791–795.
16. V. V. Belaga *et al.*, *Phys. At. Nucl.* **59** (1996) 1198–1200.